Dynamic interaction of Norfloxacin to Magnesium Monitored by Bacterial Outer Membrane Nanopores

Jiajun Wang [1, #], Jigneshkumar Dahyabhai Prajapati [3, #], Ulrich Kleinekathöfer [3], Mathias Winterhalter* [2]

1. State Key Laboratory of Analytical Chemistry for Life Science, School of Chemistry and Chemical Engineering, Nanjing University, Nanjing 210023, China
2. Department of Life Sciences and Chemistry, Jacobs University, Bremen, 28759, Germany
3. Department of Physics and Earth Sciences, Jacobs University Bremen, 28759 Bremen, Germany.

[#] These authors contribute equally.

KEYWORDS: Outer membrane porins, fluoroquinolone, nanopore, single molecule analysis, Brownian dynamic simulation, electrophysiology

ABSTRACT

The effect of divalent ions on the permeability of norfloxacin across the major outer membrane channels from *E. coli* (OmpF, OmpC) and *E. aerogenes* (Omp35, Omp36) has been investigated at the single channel level. To understand the rate limiting steps in permeation, we reconstituted single porin into planar lipid bilayers and analyzed the ion current fluctuations caused in the presence of norfloxacin. To obtain an atomistic view, we complemented the experiments with millisecond-long free energy calculations based on temperature-accelerated Brownian dynamics simulations to identify the most probable permeation pathways of the antibiotics through the respective pore. Both, experimental analysis and computational modelling, suggest that norfloxacin is able to permeate through the larger porins, i.e., OmpF, OmpC, and Omp35, whereas it only binds to the slightly narrower porin Omp36. Moreover, divalent ions can bind to negatively charged residues inside the porin, reversing the ion selectivity of the pore. In addition, the divalent ions can chelate with the fluoroquinolones and alter their physicochemical properties. The results suggest that the conjugation must break with either one of them when the antibiotics molecules bypass the lumen of the porin, with the conjugation to the antibiotic being more stable than that to the pore. In general, the permeation or binding process of fluoroquinolone in porins occurs irrespective of the presence of divalent ions, but the presences of divalent ions can vary the kinetics significantly.

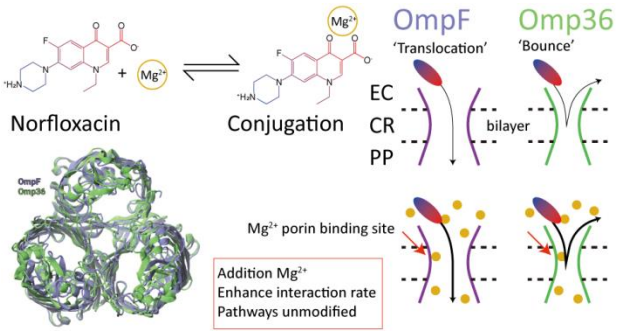

Introduction

The widespread presence of multidrug resistance (MDR) combined with the lack of new antimicrobial agents entering the market leads to an urgent need for novel antibiotics.[1] One of the current bottlenecks in the development of molecules active against Gram-negative bacteria is their low permeability across the bacterial cell wall [2, 3]. In addition to an inner membrane, the cell walls of Gram-negative bacteria possess an additional hydrophobic membrane, the so-called outer membrane (OM), which is composed of lipopolysaccharides in the outer and phospholipids in the inner leaflet.[3] Compared to Gram-positive bacteria lacking the OM, this additional layer acts as a significant barrier for hydrophilic solutes. Pore forming proteins in the OM and especially the general diffusion channels also called “porins”, e.g., OmpF and OmpC from *E. coli*, facilitate the diffusion of hydrophilic nutrients and are slightly cation selective from both in situ and in silico characterization [4-6].These porins are known to have a significant role in the influx of several classes of antibiotics, as shown by recent studies based on viability assays [7], electrophysiological characterizations [8-10] and *in silico* studies [11, 12]. Therefore, down-regulating the expression of these porins is often a prime mechanism chosen by bacteria to achieve resistance to many drugs [4, 13].

Despite its importance, so far only a few approaches are available to quantify the uptake of antibiotics molecules. The presently most widely accepted one is mass spectrometry which, however, requires a sufficient number of molecules to translocate before being able to detect the uptake [14-16]. Thus, bacteria have to be grown, soaked and subsequently the permeated molecules have to be carefully separated. To avoid the separation step, the uptake can also be studied at the single cell level using autofluorescent molecules [14].

In this study, we use electrophysiology to characterize the transport across single

porins. To this end, we titrate antibiotics on one side and the subsequent permeation of individual antibiotics molecules will transiently interrupt the ion current [10]. To get a molecular view, these electrophysiology experiments can be complemented with molecular dynamics (MD) simulations using enhanced sampling methods, e.g., umbrella sampling or metadynamics simulations [17, 18]. Such simulations have been tremendously useful to understand the transport mechanisms of solutes through nanopores in the past decade [11, 19]. In this context, we employ our recently developed temperature accelerated Brownian dynamics (TABD) approach [12, 20] to investigate the passage of fluoroquinolones and especially norfloxacin across the bacterial outer membrane porins from *E. coli* (OmpF, OmpC) and *E. aerogenes* (Omp35, Omp36) [21]. Quinolones belong to one of the most commonly prescribed classes of anti-microbials in clinics. These synthetic broad-spectrum antibiotics are effective by inhibiting the action of DNA gyrase/topoisomerase on the bacterial DNA and have to effectively cross the outer as well as the inner membrane to reach their lethal dose.[22] To complement the experiments more rigorously, we also apply external electric field during the TABD simulations, which have been included on only few occasions in free energy calculations in the past [11, 23, 24]

To obtain an enhanced understanding of antibiotics uptake, we compare the pathways of norfloxacin through four major porins, i.e., two from *E.coli* [25] and two from *E.aerogenes*. Inspection of the crystal structures [21] of these pores results in very similar architectures including the distribution of charged amino acids in the CR (Figs. 1A and B). However, viability assays [26, 27] and biophysical characterizations[28, 29] suggest that the interactions of antibiotic molecules with OmpF and the slightly smaller OmpC differ significantly. Moreover, divalent ions do have a significant effect on the antibiotic activity and thus we particularly focus on their effect on the translocation of antibiotics [30, 31].

Our experimental and computational results suggest that norfloxacin passes through

OmpF, Omp35 and OmpC but only binds and bounces back from the slightly narrower Omp36 channel. Divalent magnesium ions can bind at negatively charged residues in the CR of the porins reversing the ion selectivity. At the same time, magnesium ions can also chelate with the fluoroquinolone molecules inducing difference in the dipole moment of the respective complex causing a significant alteration in the interaction with the pores.

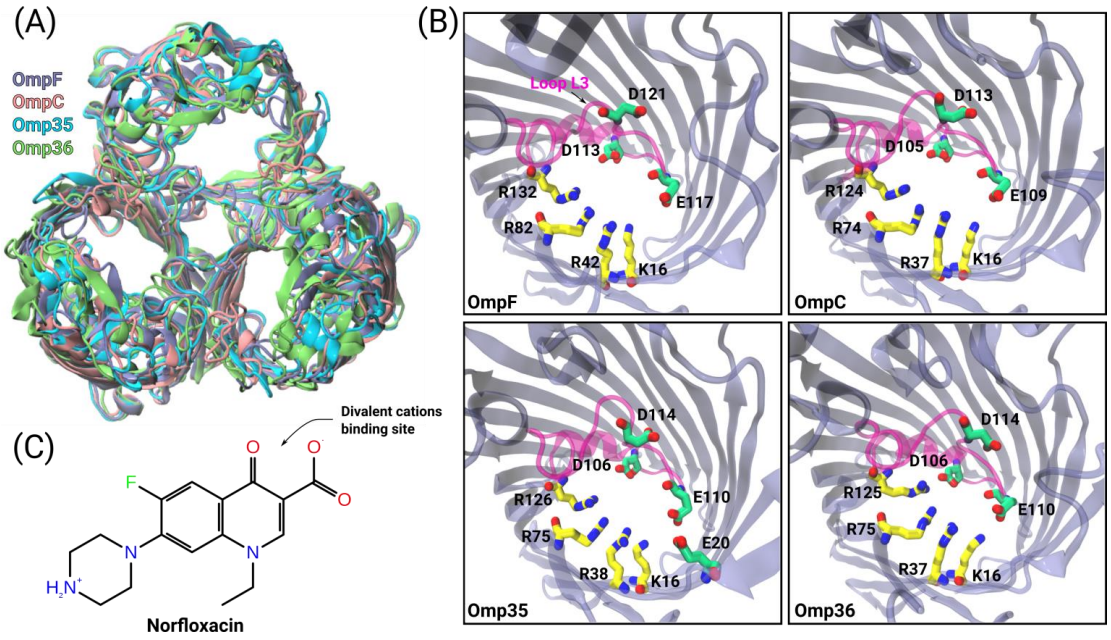

Figure 1: Structural features of the OM porins and the norfloxacin molecule. (A) The structural alignment of the four trimeric OM porins OmpF (PDB ID: 2ZFG) [32], OmpC (PDB ID: 2J1N) [33], Omp35 (PDB ID: 5O78) [21], and Omp36 (PDB ID: 5O9C) [21] is illustrated in cartoon representation. (B) Top view of the monomers in cartoon representation with the loop L3 folded into the constriction region highlighted in magenta. The negatively charged residues (C atoms: green and O atoms: red) located on loop L3 and the positively charged residues (C atoms: yellow and N atoms: blue) on the opposite barrel wall are shown as sticks. (C) 2D structure of norfloxacin in its zwitterionic configuration. The binding site of divalent ions near the carboxyl group is shown as well [31].

Results and Discussions

Ion conductance of OmpF, OmpC, Omp35 and Omp36

As a first step, the ionic permeation through all four porins in absence and presence of divalent ions has been studied (see section 1.2 of the SI for Materials and Methods). The conductance of the porins was measured by reconstituting single channels into lipid bilayers in the presence of a symmetric salt concentration on both sides of the membrane. Subsequently, transmembrane potentials of ±50 mV were applied and the ion flux through the porins was measured (see Fig. S1 in the SI). In agreement with previous studies,[25] we obtained conductance values in 1 M KCl and buffered at pH 7 of about 4.1 ± 0.4 pS (OmpF), 2.7 ± 0.3 pS (OmpC), 4.3 ± 0.5 pS (Omp35), and 3.1 ± 0.2 pS (Omp36). Note that the higher conductance values of OmpF and Omp35 compared to those of OmpC and Omp36 suggest a larger pore size which is consistent with the crystal structures. It is interesting to note that Omp36 having a slightly smaller diameter than OmpC shows a higher conductance [21].

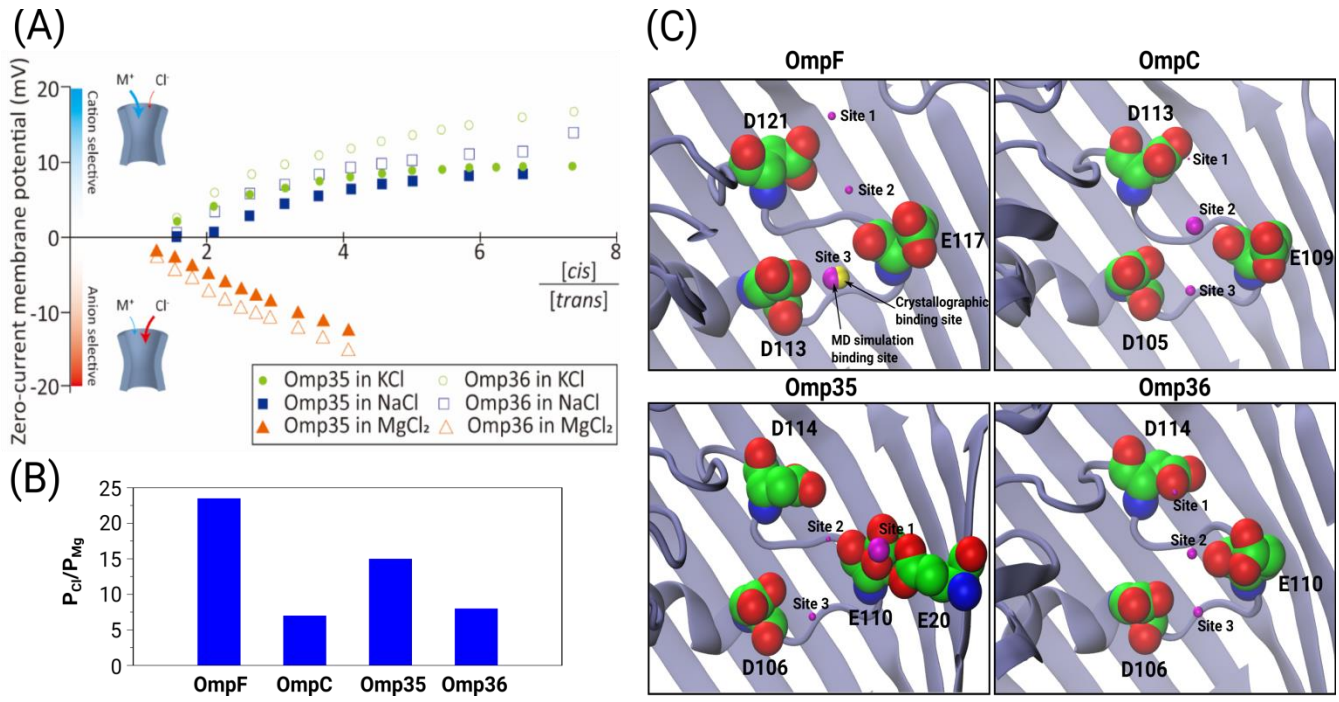

Figure 2 (A) Zero-current membrane potential of the bilayer in the presence of Omp35 and Omp36 porins measured as a function of salt (KCl, NaCl, $MgCl_2$) gradient across

the membrane. The respective salt concentration at the beginning was 10 mM on both sides and then gradually titrated at the *cis* (potential extracellular) side to reach the desired concentration. Average results of three experiments with different membranes at 20 °C and pH 7 are shown. (B) For 1 M $MgCl_2$ the permeability ratio of anions to cations (P_{Cl}/P_{Mg}) is estimated for all four proteins from MD simulations performed at 0 V. (C) The top three binding sites for Mg^{2+} ions have been identified by MD simulations for all four proteins and denoted as sites 1, 2 and 3 (magenta spheres). The position of the binding sites inside the constriction region is depicted by the respective sphere, whereas the size of the sphere represents the probability of occurrence of these sites, i.e., the larger the sphere, the higher the probability. In case of OmpF, one binding site of Mg^{2+} ions was observed in the crystal structure (yellow sphere) which is identical with site 3 observed in the simulations. The acidic residues inside the constriction region are highlighted by van der Waals spheres.

Ion selectivity of OmpF, OmpC, Omp35 and Omp36

Previous ion selectivity characterizations[39] for OmpF and OmpC were repeated for consistency while for the Omp35 and Omp36 porins zero current membrane potential measurements were performed to estimate the ion selectivity (see section 1.2 of the SI for Materials and Methods). To this end, we started with symmetrical 10 mM salt concentrations on both sides of the membrane, titrated a concentrated salt solution to the ground side (*cis*, side of protein addition) and measured the reversal potential. In Fig. 2 the reversal potentials measured for the Omp35 and Omp36 porins versus the concentration gradient of the different salts are displayed. Monovalent salts (KCl and NaCl) resulted in positive whereas $MgCl_2$ resulted in negative potentials across the membrane, suggesting cation and anion selectivity in the respective cases. The quite similar behavior of the different pores is not surprising since a sequence alignment of *E. aerogenes* Omp35 and Omp36 to OmpF and OmpC from *E. coli* shows a high similarity especially at the L3 loop which forms the *CR* in the porins [34]. Moreover, the observed inversion of the pore selectively in presence of the salt $MgCl_2$ is in agreement with previous studies in case of OmpF [32, 35, 36].

To gain a molecular understanding unbiased molecular dynamics (MD) simulations

have been carried out at zero external voltage for all four porins in presence of 1M $MgCl_2$ (see section 1.4 of SI for Materials and Methods). The estimated permeability ratios of anion to cation was found to have values higher than one clearly showing that all four pores become anion selective in presence of 1M $MgCl_2$ (see Fig. 2B). Moreover, we have also identified the top three binding pockets of Mg^{2+} ions inside the CR and named them site 1, 2 and 3 (see Fig. 2C). In case of OmpF, OmpC and Omp36, the Mg^{2+} ions tend to bind at very similar positions near the three acidic residues of loop L3. These residues are denoted as top, middle and bottom residues based on their position from the EC to the PP side. Thus, site 1 is near the top acidic residue (e.g. D121 in OmpF), site 2 is between the top and the middle residue (e.g. D121 and E117 in OmpF), and site 3 is between the middle and the bottom residue (e.g. E117 and D113 in OmpF). Remarkably, site 3 is identical to that one observed in a crystal structure of OmpF (PDB ID: 2ZFG) and found to be the most probable in the simulations [32]. Omp35 also has sites 2 and 3 like the other porins but site 1 was found at a different position due to the presence of an additional acidic residue (E20) on the barrel wall (see Fig. 1B). This Mg^{2+} binding site is also found to be the most abundant one in Omp35. Moreover, the insight obtained in terms of the binding sites was further used in the BD simulations (described below) to understand the influence of Mg^{2+} ions on the norfloxacin translocation through porins.

Permeation of norfloxacin through OmpF, OmpC, Omp35 and Omp36

The protocol to measure norfloxacin translocation is similar to that described above for ion permeation (see section 1.2 of SI for Materials and Methods). After reconstitution of a single trimer into a planar bilayer, application of transmembrane voltages of 50 mV at 1M KCl created silent current traces further used as control (Fig. S2 in SI). Addition of 0.25 mM norfloxacin on the *cis* (corresponding to the extracellular) side induced short ion current blockages.

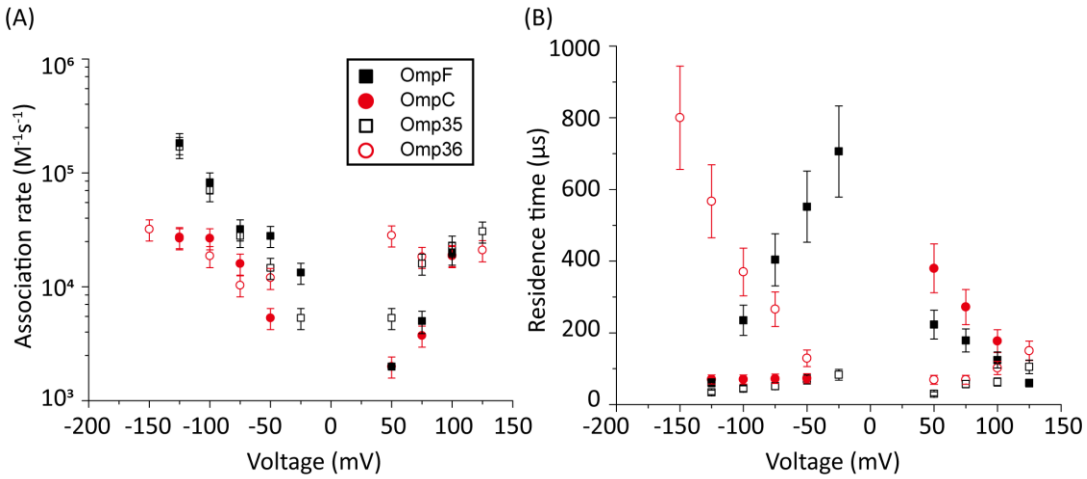

Figure 3. Voltage-dependent interaction of 0.25 mM norfloxacin with the respective porins. Addition of norfloxacin at the *cis* side, i.e., the putative extracellular side. (A) Association rate. (B) Residence time. Experiment conditions were 1 M KCl, 10 mM HEPES, pH 7.0.

To gain insight into the mode of translocation, the bias voltages was varied in the range of -150 to 150 mV. The association rates (k_{on}) and residence times (τ) were estimated as described previously[42] and shown in Fig. 3. In agreement with previous measurements for norfloxacin and OmpF, k_{on} increases exponentially with respect to the transmembrane potential at negative polarities [11]. Moreover, the voltage-dependent increase in the k_{on} rate was very similar between OmpF (or OmpC) and its ortholog Omp35 (or Omp36), suggesting that the molecules tend to approach the constriction region in a similar manner. A second parameter important for the interpretation of the data is the voltage dependence of the residence time τ. In agreement with previous measurements [11], when increasing the negative applied voltage in magnitude, OmpF shows a very steep decrease of the residence time τ from ~750 to ~50 µs, whereas for OmpC and Omp35 we have observed only a slight reduction in τ from ~100 to ~50 µs. In contrast, for Omp36 the dwell time τ increased rapidly from ~100 to ~1000 µs with increasingly negative voltages indicating that the molecule is not able to permeate through the constriction region likely due to the steric limitations imposed by the smaller diameter of the Omp36 pore [21]. At positive

voltages, one can observe a voltage-dependent increase in the k_{on} rates for all the porins, however, the values are slightly lower than the ones observed at negative voltages. Interestingly, a decay in the residence time τ can only be observed for the OmpF and OmpC porins, whereas the values remain almost constant for Omp35 and Omp36. This finding suggests that with the application of positive voltages the permeation of norfloxacin is enhanced for OmpF and OmpC. In contrast, the permeation through Omp35 and Omp36 is slower (or maybe even vanishing) at positive voltages.

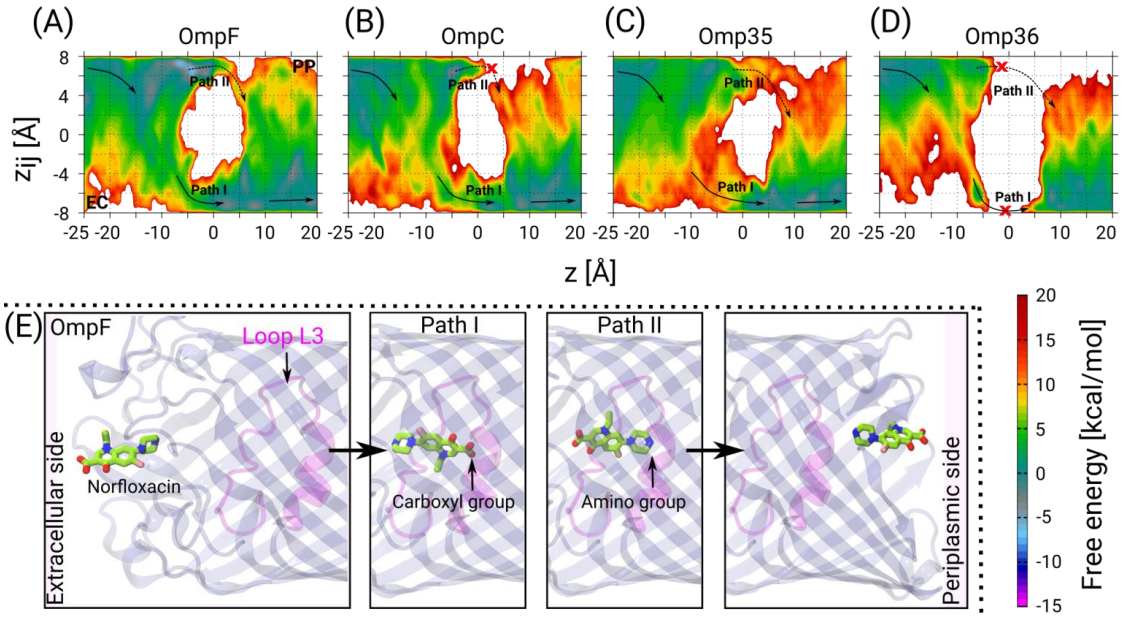

Figure 4. 2D FESs as function of the CVs z and z_{ij} from TABD simulations. The FESs for norfloxacin permeation through the four OM porins, i.e., OmpF (A), OmpC (B), Omp35 (C) and Omp36 (D), in absence of any ionic solution. The arrows indicate the most probable path which the molecules most likely take while permeating through the respective pore. The molecules can adopt two different orientations inside the constriction region depicted as Path I (solid arrows) and Path II (dotted arrows). In case of OmpC (B) and Omp36 (D) these paths are broken which is indicated by red crosses. (E) Representative conformations of norfloxacin at the EC vestibule, the CR (for Path I and II) and the PP vestibule in case of OmpF. The norfloxacin molecule is shown in stick representation (C atoms: green, N atoms: blue, O atoms: red and F atom: pink) and the protein in cartoon representation with loop L3 highlighted in magenta.

Next, we have carried out temperature accelerated Brownian dynamics (TABD) simulations in absence of external voltages to provide atomic-level understanding of the transport mechanisms of norfloxacin through all four porins (see section 1.5 of SI for Materials and Methods). The reconstructed free energy surfaces as a function of the collective variables (CVs), i.e., the position z along the pore axis and the orientation-related variable z_{ij} of norfloxacin [12, 20], are illustrated in Fig. 4. The CV z represents the position of the molecule along channel axis, where values of -25, 0 and 20 Å correspond to molecule locations at the EC (extracellular) side, the CR and the PP (periplasmic) side, respectively. The values of CV z_{ij} represent the orientation with limiting values of +8 and -8 Å which respectively correspond to the carboxyl group or the amino group facing towards the PP space, denoted as orientation I and II, respectively. The permeation pathways with these orientations are denoted as path I and II, respectively. For all four porins, we have observed that norfloxacin molecules are most likely to enter the EC side with orientation II (amino group ahead) and then orient in two different ways as they move further towards the CR, i.e., they either keep the same orientation or completely reorient to obtain orientation I (carboxyl group ahead). In general, we observed that the molecules tend to approach the CR with orientation II much more easily than with orientation I. However, further crossing through the CR is less likely to occur with orientation II in case of OmpF, OmpC, and Omp35 as the energy barrier is much higher than in case of orientation I. In conclusion, path I is the route of choice in all three porins (see Fig. 4). Interestingly, both paths are found to be disconnected in case of the Omp36 porin suggesting that the energy barriers are very high inside the CR and that permeation of norfloxacin is least likely to occur through this pore. Notably, the broken paths in case of OmpC and Omp36 suggest high energy barriers, i.e., so high that they are not sample with the present parameters. For these positions and orientations one should be able to sample the respective paths by using higher artificial temperature for the biasing CVs as shown in our previous study on the ciprofloxacin translocation through OmpC [12].

Furthermore, we have carried out TABD simulations for all four proteins in presence of various external voltages, i.e., at -200, -100, +100 and +200 mV, to illustrate voltage-dependent effects on the permeation paths and to complement the experimental results (see Fig. S3 in SI). The likelihood of a permeation event using path II, i.e., the amino group ahead, in absence of any applied voltage is largest for OmpF, followed by Omp35 and OmpC and smallest for Omp36 (see Fig. 4A). In analogy to the experiments, the application of negative voltages should enhance the probability for such an orientation along the pore due to the zwitterionic nature of molecule with a strong dipole of ~44 D. As described earlier, the rapid decay of the residence time τ observed with increasingly negative voltages in OmpF during experiments suggest that the permeation becomes much easier with orientation II (see Fig. 3). Apparently, such a behavior can be observed for simulations at -100 and -200 mV where we clearly see a progressive decrease in the energy barrier for path II and an increase in case of path I (see Fig. S3A in SI). In contrast, very small decays in the residence time τ with increasingly negative voltages in case of Omp35 and OmpC during experiments indicate that the translocation is not efficient with orientation II and remains basically unaltered with increasing external voltages. Interestingly, we have observed an increase in the sampling along path II for both porins with the application of negative voltages in the simulations, however, the change in the energy barrier height is insignificant (see Fig. S3B & C in SI). This finding suggests that the intrinsic lack of favorable interactions of the molecule with pore-lining residues along path II in OmpC and Omp35 is the primary reason why no change in the residence time τ was observed during the experiments. In case of Omp36, a very rapid increase in the residence time τ was observed in the bilayer experiments, and a very large region of path II was not sampled in absence of an external potential in simulation. Moreover, we did not observe any significant changes along path II with application of external potentials (see Fig. S3D in SI), leading to the conclusion that Omp36 most likely does not allow the transport of norfloxacin, at least in orientation II.

On the other hand, the likelihood of permeation in orientation I, i.e., the carboxyl group facing towards the PP space, in absence of any external potentials is largest for OmpF, followed by OmpC and Omp35 and is smallest for Omp36. This orientation is expected to be enhanced at positive voltages. Path I can be seen to be favorable for OmpF and OmpC in absence of external fields. A rapid decay observed in the residence time τ during experiments is clearly supporting the fact that a translocation event is more likely for orientation I with increasing positive voltages. With application of positive voltages during the simulations, one can clearly see that path I remains intact with a slight reduction in the energy barriers and path II eventually gets disconnected for both porins when the voltage reaches +200 mV (see Fig. S3A & B in SI). In case of Omp35, we have observed that in certain regions of the EC side (at z = -10 to -5 Å) along path I, the molecules face a quite high energy barrier in the absence of an external potential. With application of positive voltages, the path becomes slightly more accessible but the energy barrier remains much higher than in case of OmpF/C (see Fig. S3C in SI). Again, this intrinsic high energy barrier likely is the reason why no decrease in the residence time τ was observed in the experiments with increasing the positive voltages. Nonetheless, the molecule can still permeate at rates lower than that of OmpF/C. In Omp36, again a large region of path I is not sampled properly which means that the respective energies are too high for the present simulation parameters. This finding stays the same in the presence of external fields (see Fig. S3D in SI). Surprisingly, no change in the residence time τ was observed in the experiments at positive voltages compared to rapid increase at negative voltages. Based on the high energy barriers observed in the simulations and the unchanged residence times τ in experiment, we believe that norfloxacin cannot or only very rarely permeate through Omp36.

Our observation that norfloxacin can permeate faster through OmpF than through OmpC is consistent with earlier studies [37]. It is also in agreement with the fact that in minimum inhibitory concentration (MIC) assays for *E. coli* the deletion of OmpF leads

to higher MIC values than for the case of OmpC [38]. On other hand, there are so far no studies which clearly distinguish the role of Omp35 and Omp36 in quinolone uptake. However, it was shown that *E. aerogenes* is very less susceptible to ciprofloxacin and some other quinolones compared to *E. coli* [39]. Therefore, it is quite likely that the low permeability through the Omp35 and Omp36 porins is the reason for the poor activity of norfloxacin and other quinolones in *E. aerogenes* bacteria.

Interaction of norfloxacin with divalent ions

To characterize the affinity of Mg^{2+} ions with fluoroquinolones molecules, fluorescence assays have been performed (see section 1.3 of SI for Materials and Methods). In presence of divalent ions, norfloxacin and other fluoroquinolones chelate to form complexes. In agreement with the literature [40], at pH 7.0 we observed a shift in the fluorescence while changing the $MgCl_2$ concentration from 0.4 to 1.6 µM (see Fig. S4 in SI) suggesting that fluoroquinolones (norfloxacin, ciprofloxacin and enrofloxacin) form complexes with the Mg ions. In contrast, at pH 5, only a slight increase in the fluorescence intensity was observed (see Fig. S4 in SI). This results confirms that at pH 5 (pKa = 6.1) no complexes are formed pointing to a protonation of the carboxyl group of the antibiotic molecules [41].

Permeation of norfloxacin in presence of divalent ions

In the series of experiments described in the following, the role of divalent ions in the permeation of norfloxacin has been investigated. OmpF and Omp36 have been taken as examples since their pathways for the translocation without divalent ions differed most. At voltages in the range of -25 mV to -125 mV, increase in the k_{on} rates was observed for both porins in presence of divalent cations which is similar to the findings observed in absence of divalent ions. As shown in Fig. 5A , at -125 mV the k_{on} rates for OmpF increased from 0.15 $x10^5$ in absence of divalent ions to 6 $x10^5$ and 7 $x10^5$ $s^{-1}M^{-1}$ in the presence of 5 mM Ca^{2+} and Mg^{2+} ions, respectively. Similarly, the k_{on}

rates for Omp36 increased from 0.12 x10^5 to 2 x10^5 and 4 x10^5 $s^{-1}M^{-1}$ at -125 mV as shown in Fig. 5C. The increased k_{on} rates for both porins is assumed to be due to the conjugation of norfloxacin with the divalent ions leading to a complex with +2e net charge. Due to this net charge, the complex gets pulled from the *cis* to *trans* side of the channel when negative potentials are applied on the *trans* side leading to an increased permeation rate.

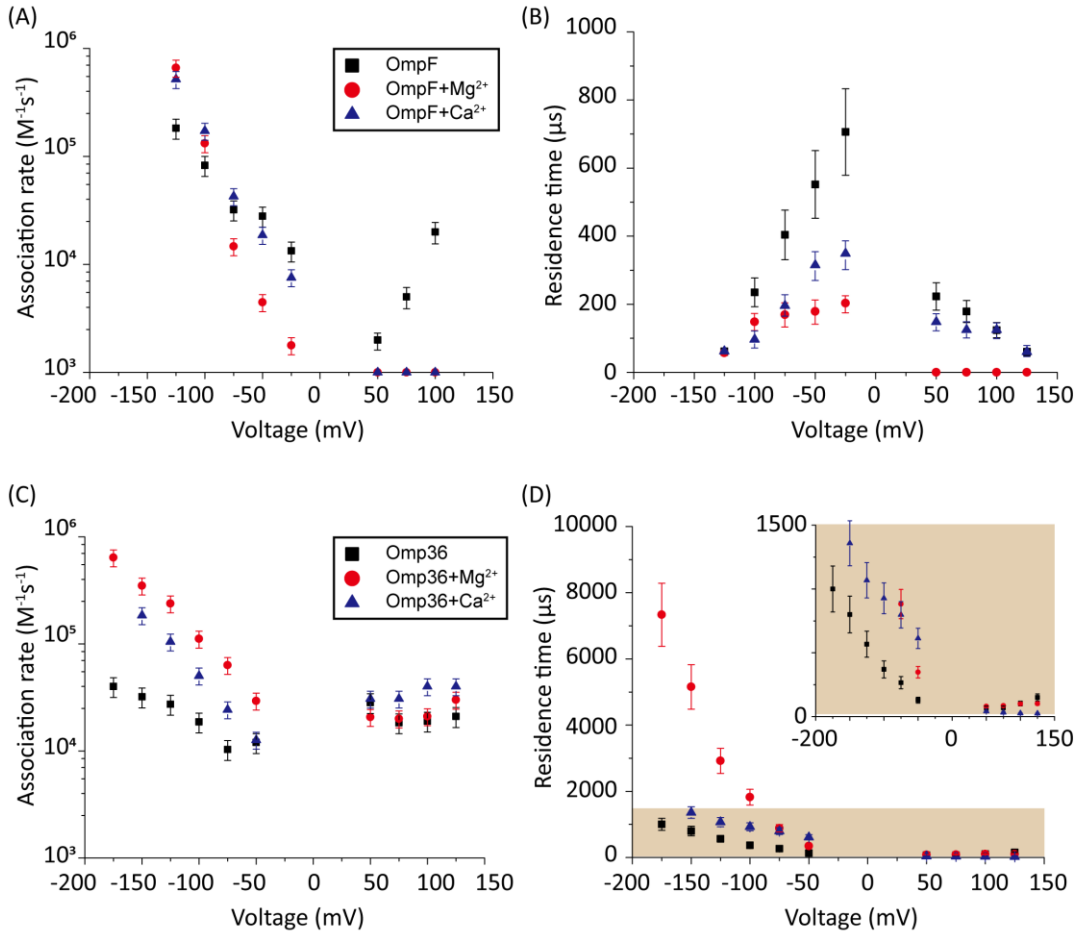

Figure 5. Voltage-dependent association rates (A) and residence time (B) on the *cis* side for the interaction of norfloxacin with the OmpF porin in presence of 1 M KCl (black squares), 1 M KCl with 5 mM $MgCl_2$ (red dots) and 1 M KCl with 1 mM $CaCl_2$ (blue triangles). Panels (C) and (D) are for the case of the Omp36 porin with the same buffer condition as in (A) and (B).

Such pulling effects for OmpF can be observed in the presence of Ca^{2+} and Mg^{2+} ions as the residence time τ for norfloxacin decreased from 400 µs to 60 µs and from 200 µs to 60 µs, respectively, when the magnitude of the negative voltage is increased from -25 mV to -125 mV (see Fig. 5B). In case of Omp36, however, increasing the magnitude of the negative voltage causes an increase of the residence time from 60 µs to 2 ms and 7 ms in the presence of Ca^{2+} and Mg^{2+} ions, respectively (see Fig. 5D). Both cases demonstrated that the addition of divalent ions causes a stronger pulling effect irrespective of the pathway. Moreover, there are no drastic alternations for both porins at positive voltages. The lower k_{on} rates and residence time values τ indicate that the positively charged chelation complexes interact less with the porins.

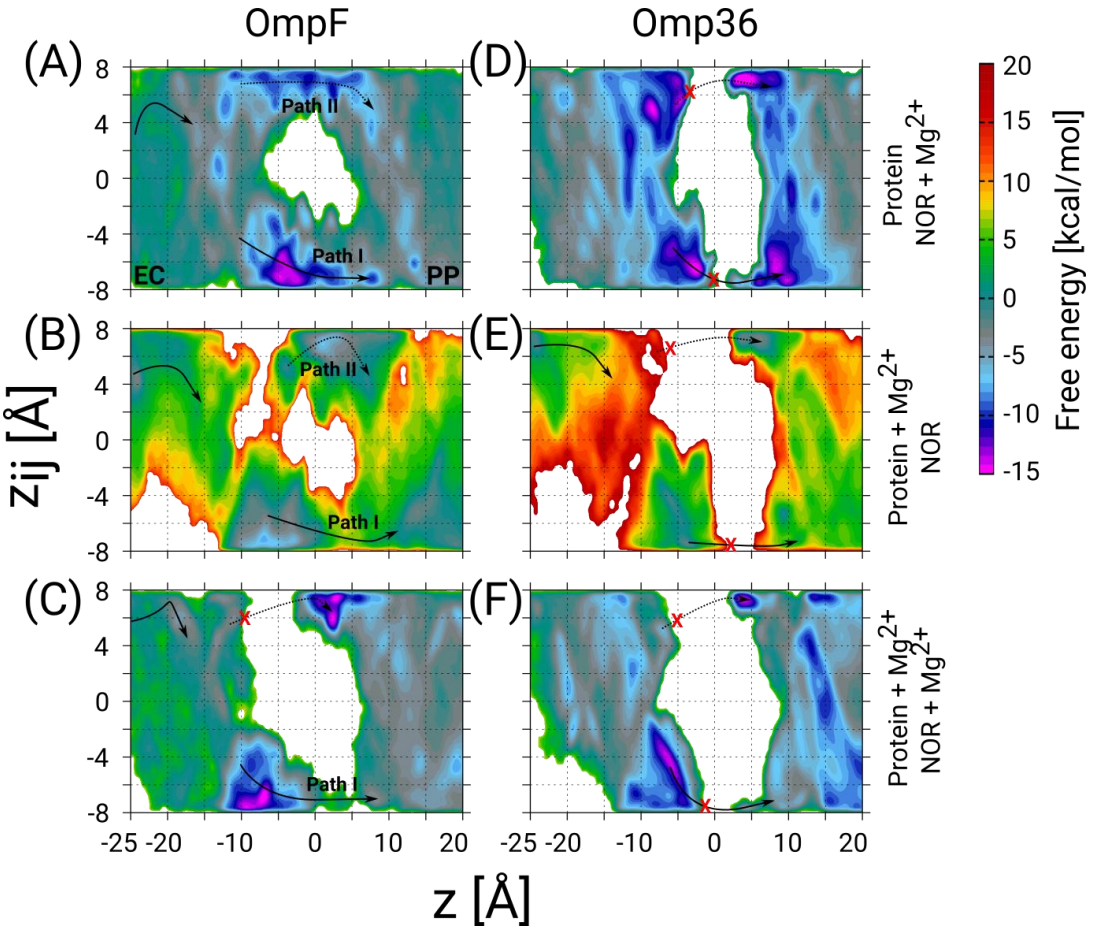

Figure 6. 2D FESs as function of the CVs *z* and z_{ij} determined using TABD simulations for OmpF and Omp36 and performed to understand the influence of Mg^{2+} ions on the norfloxacin translocation. The FESs for OmpF have been obtained for three different scenarios, i.e., Mg^{2+} ion(s) bound to (A) only norfloxacin, (B) only the porin, and (C)

both, norfloxacin and the porin. Panels D, E and F show the same but for Omp36. As in Fig. 4, the two possible paths with opposite orientation inside the constriction region are depicted as Path I and Path II with solid and dashed arrows, respectively, and broken paths are marked by red crosses.

To get further atomistic insight into the influence of divalent ions, we have carried out TABD simulations in the three most probable scenarios based on the ability of divalent ions to complex with the porin and/or the norfloxacin molecule, i.e., (i) only with norfloxacin, (ii) only with the porin, and (iii) with both, norfloxacin and the porin (see section 1.5 of SI for Materials and Methods). All these simulations together should be able to provide significant insight because in experiments one probably finds a mixture of all three cases. The estimated FESs for OmpF and Omp36 are shown in Fig. 6. In case of OmpF, both paths can be seen, i.e., path I and II with the carboxyl and the amino group ahead, receptively, when the norfloxacin molecule is complexed with an Mg^{2+} ion (see Fig. 6A). The barriers for both paths actually changed into wells with the well for path I being deeper. In case of a Mg^{2+} ion only attached to the pore but not to the norfloxacin molecule (see Fig. 6B), the respective path is slightly less accessible but path I remains intact. Finally, when Mg^{2+} ions were placed on both, i.e., the norfloxacin molecule and the pore, leading to positive charges on both, path II is broken using the present simulation parameters and the sampling around path I is significantly reduced (see Fig. 6C). It is highly likely that path I would be also disappear if more divalent ions would be present inside the CR. Since the dipole moment of norfloxacin is reduced by about 70% when complexed with a Mg^{2+} ion, the polarity of external potentials will not have a strong influence on the orientational preference (path I or II). Interestingly, one can observe a very strong interaction near the constriction region when the molecule follows path I (between z = -10 to 0 Å) in all three scenarios, especially for the conjugated norfloxacin molecule, indicating that divalent ions intrinsically enhance the affinity of norfloxacin to the CR independent of where it binds. However, the permeation through the CR would become difficult when divalent ions bind to both, the molecule and the pore, which is likely to occur.

Therefore, one of the complexes has to break in order to make permeation more feasible. Based on the experimental data obtained at negative and positive voltage polarities, we argue that the complex with norfloxacin remains quite intact compared to the one with the pore. Therefore, we have observed an increase in the k_{on} rate and a decrease in the residence time τ with negative applied voltages as the molecule in its conjugated form with net charge +2e gets pulled along the pore.

In case of Omp36, the results in the CR along both possible paths for all three scenarios in terms of Mg^{2+} ion binding (see Fig. 6D, E & F) indicate only a rare permeation likelihood of norfloxacin. On other hand, a strong interaction of norfloxacin can be observed near the CR (at z = -10 to -5 Å) similar to the case of OmpF. This result supports the very high residence times τ observed in the experiments displayed in Fig. 5. Overall, it can be concluded that the molecules can strongly interact within the CR but permeation is unlikely to happen across Omp36 also in the presence of divalent cations.

Moreover, in the experiments using OmpC and Omp35 we have seen an increase in the k_{on} rates (see Fig. S5 in the SI). The change in the residence times τ, however, was not drastic, i.e., a slight increase for OmpC from 90 to 200 µs and a moderate decrease for Omp35 from 100 to 60 µs. These findings differ from the drastic changes observed for OmpF and Omp36. Furthermore, the simulations also suggest that Mg^{2+} ions clearly influence the permeation paths for OmpC and Omp35 (see Fig. S6 in the SI) enforcing strong interactions with the pore when complexed with the molecule. In general, the behavior was quite similar to that of OmpF, i.e., either path I or II was accessible depending on where Mg^{2+} ions bind. A major difference was observed in Omp35 when the Mg^{2+} ions bind to the pore only. In that case, path II becomes more accessible. Due to the tendency of Mg^{2+} ions in Omp35 to bind at different positions compared to other porins, i.e., site 1 which was found near residue E20, the molecule orients with the amino group facing towards the PP space (path II). Overall, based on

the experiments and the simulations, we suggest that permeation of norfloxacin should be possible through OmpC and Omp35 in presence of divalent cations without drastic change in kinetics.

Magnesium concentration effect the interaction kinetics

In the following set of experiments we analyzed the effect of Mg^{2+} ion concentration on the k_{on} rate and the residence time τ for norfloxacin interactions with OmpF and Omp36. As shown in Fig. 7, the increase of the Mg^{2+} ions concentration from 10 µM to 5 mM induces an increase of the k_{on} rates for both, OmpF ($2x10^4$ $s^{-1}M^{-1}$ to $10x10^4$ $s^{-1}M^{-1}$) and Omp36 ($5x10^4$ $s^{-1}M^{-1}$ to $10x10^4$ $s^{-1}M^{-1}$). The τ values for OmpF (400 µs to 60 µs) keep decreasing while they increase for Omp36 (1 ms to 2 ms). Interestingly, this trend is similar to that observed in voltage-dependent experiments shown in Fig. 5.

Analyzing the magnesium concentration dependence in more detail shows that the k_{on} rates for both porins increases in a steady manner. The rise is small in the concentration range from 10 µM to 250 µM and then becomes drastically larger until 5 mM. Notably, this sudden change in the kinetic constants appears when the concentration of Mg^{2+} ions becomes equivalent to that of the norfloxacin molecules, i.e., 250 µM. This coincidence indicates that if concentration of Mg^{2+} is lower than that of norfloxacin, less chelates are formed and therefore less change in the k_{on} values can be observed at negative applied negative voltages. But as the concentration of the Mg^{2+} ions surpasses that of the norfloxacin molecules, the probability to form chelates is rapidly increased resulting in a fast enhancement of the k_{on} values. On the other hand, the concentration-dependent decay in the residence time τ for OmpF supports the fact that the chelate formation increases the permeability of norfloxacin through OmpF. It must be noted that the increase in the number of Mg^{2+} ions also increases their tendency to bind to pore, which is expected to slow down the permeation of norfloxacin as shown in simulations. However, the steady decay in

residence time τ suggests otherwise. That must be due to our earlier claim that the conjugated form of the molecule remains intact and the Mg^{2+} ions get cleaved from the CR of the pore more easily during the permeation process through OmpF, especially because the presence of external voltages. Interestingly, the τ values for Omp36 increase for increasing Mg^{2+} ion concentrations below 250 μM, and remain unchanged above this concentration. It is quite clear that with the formation of more chelates outside the pore, more molecules approach the pore and bind strongly to the CR, but as the molecules do not permeate through the pore, further addition of Mg^{2+} ions does not improve the binding ability with the pore. Overall, considering the results for both porins, it is evident that magnesium ions clearly changes the kinetics of norfloxacin molecules, irrespective of the fact if they permeates or just binds to the pore.

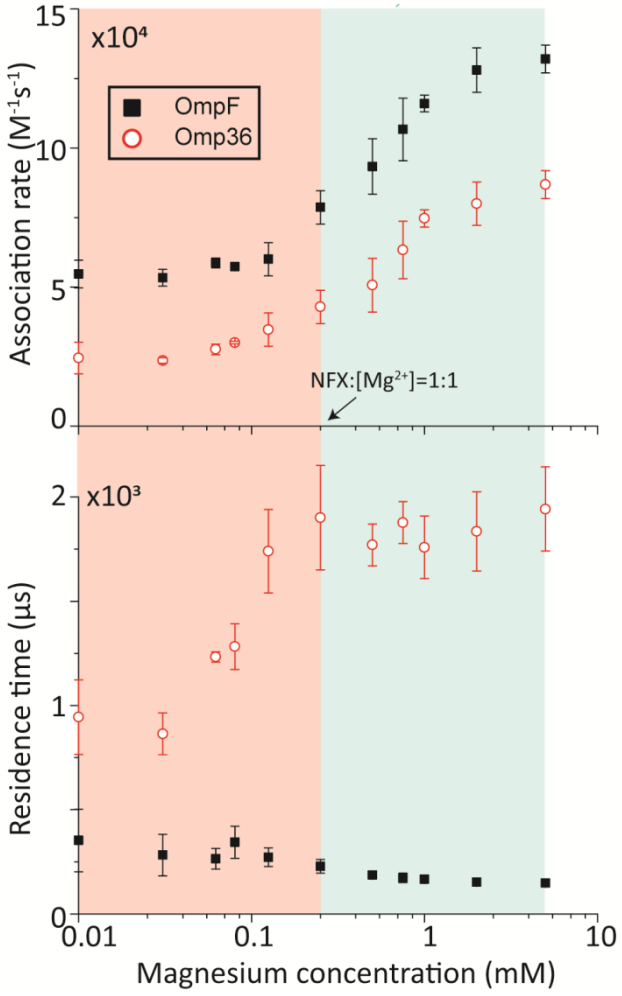

Figure 7. OmpF and Omp36 interaction with 250 µM norfloxacin (*cis* addition) as function of the $MgCl_2$ concentration at pH 7 with a -100 mV potential. The association rate calculated from the single channel interactions is shown in the upper panel and the residence time is plotted in the lower panel.

Conclusions

The permeation of norfloxacin across four homologous channels from *E. coli* (OmpF, OmpC) and *E. aerogenes* (Omp35, Omp36) have been studied with a special focus on the effectof additional divalent ions. The experiments have been conducted in absence and presence of divalent ions in order to illustrate their influence on the permeation process. The effect of divalent ions is investigated due to the physiological relevance to the bacterial OM, e.g., divalent ions are present in LPS membranes and thus also within the porins surrounded by LPS molecules. As shown in a crystallographic structure of OmpF, these divalent ions can bind to the pore lining residues. Moreover, atomistic insights into the underlying permeation pathways have been obtained by virtue of free energy calculations using the TABD simulation technique.

As one important point we addressed which of the four studied porins facilitate the permeation of norfloxacin molecules in absence of divalent ions. Based on the experiments and simulations results, we conclude that OmpF, which has the largest pore diameter, allows the most efficient permeation of norfloxacin irrespective of magnitude and polarity of external voltages. Its orthologue Omp35 and homologue OmpC are less efficient and might not facilitate the permeation of norfloxacin for all external voltages. The porin Omp36, however, seems not to be suitable for norfloxacin transport due to its pore diameter which is slightly smaller than that of the three other porins. Nonetheless, the molecule approaches and binds to the Omp36 pore in a similar fashion as to the three proteins. At the same time, norfloxacin cannot translocate through Omp36 but bounces back to the same membrane side from which

it originated.

Furthermore, we have demonstrated that divalent ions have a strong affinity with the norfloxacin molecule and CR residues of the pore using fluorescence assays and reversal potential measurements, respectively. With the introduction of divalent ions in single channel experiments, we have observed a strong increase in the association rates for norfloxacin with all four porins at one polarity of external voltages, indicating improved approachability of the molecule to the CR. Such a behavior was also observed during the simulations in which the molecule bind with a strong affinity to the conjugated form, especially when the carboxyl group of the molecule with Mg^{2+} bound faces towards the CR. The subsequent crossing from the CR to the periplasmic vestibule remains possible in case of three porins, i.e., OmpF, OmpC and Omp35, as already observed in absence of divalent ions. Based on our findings, we suggest that the complexes of divalent ions with norfloxacin molecules have a stronger internal binding than the ions with the CR of pore during the permeation process. For Omp36, a crossing of the CR is still not possible even though divalent ions improve the binding affinity. Overall, we conclude that divalent ions improve the affinity of norfloxacin with all pores. Moreover, they do not alter the permeation process through OmpF, OmpC and Omp35 as well as the binding and bouncing back process in case of Omp36, though changes in the kinetic rates can clearly be seen.

In terms of technical advancement, we have presented an application of external voltages in free energy calculations to support experimental outcomes thoroughly. Moreover, we also demonstrate the influence of divalent ions on antibiotics permeation which is not often neglected in past. On one hand, MD simulations allows more accurate and realistic simulations of OM porins, e.g. by inclusion lipopolysaccharides and ions [42]. However, on other hand, influence of voltages is not easy to study in MD simulations due to tremendous need of computational resources. Thereby, TABD simulations can be used alone or in parallel to MD simulations to gain

better atomistic insight in future. Additionally, such simulations could have a great impact in the future to complement single channel electrophysiology experiments which are based on applying of external bias potentials. With the combination of electrophysiology experiments and molecular simulations, one can improve the understanding of permeation mechanisms of existing antibiotics through OM porins at the atomistic scale which will help to improve the design of next generation antimicrobials.

Supporting information

Intensity of fluorescence of norfloxacin, ciprofloxacin and enrofloxacin with magnesium at pH 5.0 and pH 7.0. Current trances from single channel recording in presence and absence of norfloxacin for all four porins in 1 M KCl. TABD simulations for norfloxacin permeation through all four porins in absence of ionic salts and in presence of applied voltages. Single channel recordings of Omp35 and Omp36 with norfloxacin in presence and absence of $MgCl_2$. TABD simulation in presence Mg^{2+} ions for norfloxacin permeation through Omp35 and OmpC. Details on material and methods.

Note

All authors declare no competing financial interest.

ACKNOWLEDGMENT

The authors would like to acknowledge Prof. Dr. Jean-Marie Pagès (Faculté de Médecine, Aix-Marseille Université, Marseille, France) for providing the purified proteins Omp35 and Omp36. This work has received support from the Innovative Medicines Initiative Joint Undertaking under Grant Agreement no. 115525, resources

which are composed of financial contribution from European Union seventh framework programme (FP7/2007-2013) and EFPIA companies. We further acknowledge support from EU FP7-PEOPLE-2013-ITN, Marie-Skłodowska Curie Translocation network Nr. 607694. JW is sponsored by National Natural Science Foundation of China (61901171). Moreover, financial support by the Deutsche Forschungsgemeinschaft (DFG) through project KL1299/9-2 is gratefully acknowledged.

Reference

1. Martínez-Martínez, L., Pascual, A. & Jacoby, G.A. Quinolone resistance from a transferable plasmid. *The Lancet* **351**, 797-799 (1998).

2. Stavenger, R.A. & Winterhalter, M. TRANSLOCATION project: how to get good drugs into bad bugs. *Science translational medicine* **6**, 228ed227-228ed227 (2014).

3. Vergalli, J. *et al.* Porins and small-molecule translocation across the outer membrane of Gram-negative bacteria. *Nature Reviews Microbiology* **18**, 164-176 (2020).

4. Nikaido, H. Molecular Basis of Bacterial Outer Membrane Permeability Revisited. *Microbiology and Molecular Biology Reviews* **67**, 593-656 (2003).

5. Alcaraz, A., Nestorovich, E.M., Aguilella-Arzo, M., Aguilella, V.M. & Bezrukov, S.M. Salting out the ionic selectivity of a wide channel: the asymmetry of OmpF. *Biophys. J.* **87**, 943-957 (2004).

6. Im, W. & Roux, B. Ion permeation and selectivity of OmpF porin: a theoretical study based on molecular dynamics, Brownian dynamics, and continuum electrodiffusion theory. *Journal of Molecular Biology* **322**, 851-869 (2002).

7. Chevalier, J., Mallea, M. & Pages, J.-M. Comparative aspects of the diffusion of norfloxacin, cefepime and spermine through the F porin channel of Enterobacter cloacae. *Biochemical Journal* **348**, 223-227 (2000).

8. Vikraman, D., Satheesan, R., Kumar, K.S. & Mahendran, K.R. Nanopore Passport Control for Substrate-Specific Translocation. *ACS Nano* **14**,

2285-2295 (2020).

9. Danelon, C., Nestorovich, E.M., Winterhalter, M., Ceccarelli, M. & Bezrukov, S.M. Interaction of zwitterionic penicillins with the OmpF channel facilitates their translocation. *Biophys. J.* **90**, 1617-1627 (2006).

10. Wang, J., Bafna, J., Bhamidimarri, S.-P. & Winterhalter, M. Small molecule permeation across membrane channels: Chemical modification to quantify transport across OmpF. *Angewandte Chemie International Edition* **58**, 4737 (2019).

11. Bajaj, H. *et al.* Bacterial outer membrane porins as electrostatic nanosieves: exploring transport rules of small polar molecules. *ACS Nano* **11**, 5465-5473 (2017).

12. Prajapati, J.D., Fernández Solano, C.J., Winterhalter, M. & Kleinekathöfer, U. Characterization of ciprofloxacin permeation pathways across the porin OmpC using metadynamics and a string method. *Journal of chemical theory and computation* **13**, 4553-4566 (2017).

13. Page, M.G.P. in IMI, ND4BB (Bremen; 2016).

14. Dumont, E. *et al.* Antibiotics and efflux: combined spectrofluorimetry and mass spectrometry to evaluate the involvement of concentration and efflux activity in antibiotic intracellular accumulation. *Journal of Antimicrobial Chemotherapy* **74**, 58-65 (2019).

15. Charretier, Y. & Schrenzel, J. Mass spectrometry methods for predicting antibiotic resistance. *Proteomics. Clinical applications* **10**, 964-981 (2016).

16. Robertson, J.W.F. *et al.* Single-molecule mass spectrometry in solution using a solitary nanopore. *Proc. Natl. Acad. Sci. U. S. A.* **104**, 8207-8211 (2007).

17. Pothula, K.R., Solano, C.J. & Kleinekathofer, U. Simulations of outer membrane channels and their permeability. *Biochimica et biophysica acta* **1858**, 1760-1771 (2016).

18. Samsudin, F. & Khalid, S. Movement of Arginine Through OprD: The Energetics of Permeation and The Role of Lipopolysaccharide in Directing Arginine to The Protein. *The Journal of Physical Chemistry B* (2019).

19. Golla, V.K. *et al.* Fosfomycin Permeation through the Outer Membrane Porin OmpF. *Biophys J* **116**, 258-269 (2019).

20. Solano, C.J., Prajapati, J.D., Pothula, K.R. & Kleinekathöfer, U. Brownian Dynamics Approach Including Explicit Atoms for Studying Ion Permeation and Substrate Translocation across Nanopores. *Journal of chemical theory and computation* **14**, 6701-6713 (2018).

21. Acosta-Gutierrez, S. *et al.* Getting drugs into Gram-negative bacteria: Rational rules for permeation through general porins. *ACS infectious diseases* **4**, 1487 (2018).

22. Walsh, C. *Antibiotics*. (American Society of Microbiology, 2003).

23. Reale, R. *et al.* Human aquaporin 4 gating dynamics under and after nanosecond-scale static and alternating electric-field impulses: a molecular dynamics study of field effects and relaxation. *J Chem Phys* **139**, 205101 (2013).

24. Napolitano, L.M. *et al.* A structural, functional, and computational analysis suggests pore flexibility as the base for the poor selectivity of CNG channels. *Proc Natl Acad Sci U S A* **112**, E3619-3628 (2015).

25. Cowan, S. *et al.* Crystal structures explain functional properties of two E. coli porins. *Nature* **358**, 727-733 (1992).

26. Masi, M. & Pagès, J.-M. Structure, Function and Regulation of Outer Membrane Proteins Involved in Drug Transport in Enterobactericeae: the OmpF/C – TolC Case. *The Open Microbiology Journal* **7**, 22-33 (2013).

27. Redgrave, L.S., Sutton, S.B., Webber, M.A. & Piddock, L.J. Fluoroquinolone resistance: mechanisms, impact on bacteria, and role in evolutionary success. *Trends in Microbiology* **22**, 438-445 (2014).

28. Prajapati, J.D., Solano, C.J.F., Winterhalter, M. & Kleinekathofer, U. Enrofloxacin Permeation Pathways across the Porin OmpC. *The journal of physical chemistry. B* **122**, 1417-1426 (2018).

29. Cama, J. *et al.* Quantification of fluoroquinolone uptake through the outer membrane channel OmpF of Escherichia coli. *Journal of the American Chemical Society* **137**, 13836-13843 (2015).

30. Alkaysi, H., Abdel-Hay, M., Salem, M.S., Gharaibeh, A. & Na'was, T. Chemical and microbiological investigations of metal ion interaction with norfloxacin. *International journal of pharmaceutics* **87**, 73-77 (1992).

31. Bax, B.D. *et al.* Type IIA topoisomerase inhibition by a new class of antibacterial agents. *Nature* **466**, 935 (2010).

32. Yamashita, E., Zhalnina, M.V., Zakharov, S.D., Sharma, O. & Cramer, W.A. Crystal structures of the OmpF porin: function in a colicin translocon. *Embo Journal* **27**, 2171-2180 (2008).

33. Baslé, A., Rummel, G., Storici, P., Rosenbusch, J.P. & Schirmer, T. Crystal Structure of Osmoporin OmpC from E. coli at 2.0 Å. *Journal of Molecular Biology* **362**, 933-942 (2006).

34. Bornet, C. *et al.* Omp35, a new Enterobacter aerogenes porin involved in selective susceptibility to cephalosporins. *Antimicrobial Agents and Chemotherapy* **48**, 2153-2158 (2004).

35. van den Berg, B., Prathyusha Bhamidimarri, S., Dahyabhai Prajapati, J., Kleinekathöfer, U. & Winterhalter, M. Outer-membrane translocation of bulky small molecules by passive diffusion. *Proceedings of the National Academy of Sciences* **112**, E2991-E2999 (2015).

36. García-Giménez, E., Alcaraz, A. & Aguilella, V.M. Divalent metal ion transport across large biological ion channels and their effect on conductance and selectivity. *Biochemistry research international* **2012** (2012).

37. Mahendran, K.R., Kreir, M., Weingart, H., Fertig, N. & Winterhalter, M. Permeation of antibiotics through Escherichia coli OmpF and OmpC porins: screening for influx on a single-molecule level. *Journal of biomolecular Screening* **15**, 302-307 (2010).

38. Mortimer, P.G. & Piddok, L.J. The accumulation of five antibacterial agents in porin-deficient mutants of Escherichia coli. *Journal of Antimicrobial Chemotherapy* **32**, 195-213 (1993).

39. Sirot, J. *et al.* Susceptibility of Enterobacteriaceae to beta-lactam agents and fluoroquinolones: a 3-year survey in France. *Clinical microbiology and infection : the official publication of the European Society of Clinical Microbiology and Infectious Diseases* **8**, 207-213 (2002).

40. Vergalli, J. *et al.* Fluoroquinolone structure and translocation flux across bacterial membrane. *Scientific reports* **7**, 9821 (2017).

41. Gu, C. & Karthikeyan, K. Sorption of the antimicrobial ciprofloxacin to aluminum and iron hydrous oxides. *Environmental science & technology* **39**,

9166-9173 (2005).

42. Lee, J., Pothula, K.R., Kleinekathofer, U. & Im, W. Simulation Study of Occk5 Functional Properties in Pseudomonas aeruginosa Outer Membranes. *The journal of physical chemistry. B* **122**, 8185-8192 (2018).